한국지반공학회논문집 제17권 6호 2001년 12월 pp. 85 ~ 98

An Analysis of Cone Penetration Based on Arbitrary Larangian-Eulerian Method

Arbitrary Lagrangian-Eulerian 기법에 의거한 콘 관입 해석

Oh, Se-Boong* 오 세 붕

요 지

Arbitrary Lagrangian-Eulerian(ALE) 기법에 의거하여 콘 관입문제를 해석하였다. 완전한 관입을 모의하기 위하여 ABAQUS/Explicit을 이용하여 지반의 상향 유동을 모델링하는 정상상태해석(steady state analysis)을 수행하였다. 단일 지층의 해석에서는 흙 입자의 유동 경로와 변형률이 strain path method와 일관된 결과를 나타내고 있음을 확인하였고 극한저항을 합리적으로 계산할 수 있었다. 상이한 지층에 콘을 관입하는 경우에 대해서도 콘 저항이 전이하는 경향을 해석할 수 있었다. 따라서 ALE 해법의 정상상태해석으로 층상 지층에 대한 완전한 관입을 해석할 수 있었다.

Abstract

Cone penetration was analyzed by arbitrary Lagrangian-Eulerian(ALE) method. In order to simulate full penetration, steady state analyses were performed using ABAQUS/Explicit, which models upward flow of soil layers. In the analysis of homogeneous layer it was found that the paths and the strain of soil particles were consistent with the result of the strain path method and that the ultimate resistance were reasonably evaluated. The cone penetration through different soil layers was also analyzed and that showed the transfer of cone resistance. The steady state ALE analysis could perform full penetration through the layered soils.

Keywords : Arbitrary Lagrangian-Eulerian(ALE) method, Cone penetration, Large deformation, Strain path method

1. Introduction

In the nonlinear simulation of penetration, the soil material undergoes very large deformation. This deformation distorts the FE mesh to the point where the mesh is unable to provide accurate results or the analysis terminates for numerical reasons. For such a problem ABAQUS/Explicit version 5.8 provides an adaptive meshing technique which is based on Arbitrary Lagrangian-Eulerian (ALE) Method (HKS, 1998).

We have three sets of coordinates: spatial or Eulerian coordinates **x**, material or Lagrangian coordinates **X** and referential coordinates ξ. In a computational procedure, the referential coordinates can be used to define the nodes and elements of the mesh.

In the mesh description called *Lagrangian*, each node remains coincident with the same material particle and each element contains the same material domain throughout the deformation such that $\xi = \mathbf{X}$. Since nodes move exactly with material points in the largely deformed problem, the mesh will become distorted with high strain gradients. In the *Eulerian* mesh description,

* Member, Assistant Professor, Dept. of Civil Engrg., Yeungnam Univ.

the referential coordinate system is chosen to coincide with the spatial coordinates such that $\xi = \mathbf{x}$ and nodes stay fixed while material flows through the mesh. It is difficult to track free surface and motion of boundaries. In a Lagrangian and Euerian mesh, there is no need to introduce referential coordinate system, since the variables already play the role of referential coordinates.

Arbitrary Lagrangian-Eulerian (ALE) description can solve the disadvantages of both Lagrangian and Eulerian meshes for large deformation problems (Belytschko, 1983). A smoother mesh is generated at regular intervals to reduce element distortion and the referential coordinate is chosen so that the distortion of the mesh is distributed and reduced. Nodes on the free surface or the boundary are treated as Lagrangian. Hence, the mesh motion is somewhat independent of the material motion like the Eulerian mesh while the boundary nodes keep coincident with the material points like the Lagrangian mesh (HKS, 1998).

Recently van den Berg's (1996) solved the cone penetration on the basis of Eulerian formulation with upward flow of soil layers. Kim (2000) and Song (2001) reported the large penetration analysis of piezo-cone on the basis of updated Lagrangian formulation. Their researches include the advanced constitutive models, Bounding surface model and Cam-clay model, with coupled formulation of pore pressure and displacement. This study is on the same track as those but the solving methodology is different.

In this study ALE analyses of the cone penetration are performed through layered soil using ABAQUS. The main focus is the verification of feasibility on the ALE method for soil penetration.

2. Penetration analysis using ABAQUS/Explicit

In the conservation laws, the material time derivative of a function f is required. For example, f can be mass, linear momentum and angular momentum and is usually defined as a function of $\mathbf{x}$ and time t. In an ALE formulation ξ is prescribed or fixed, the conservation laws and their quantities are expressed in terms of ξ and t. The time derivative with the material coordinate($\mathbf{X}$) fixed is derived as follows;

$$\dot{f}(\boldsymbol{X}, t) = \frac{\partial f(\xi, t)}{\partial t} + (v_1 - \hat{v}_i)\frac{\partial f(\xi, t)}{\partial \xi_i} \qquad (1)$$

where v_i and $\hat{v}_i$ are the velocity of material and mesh. $f(\xi, t)_{,t}$ denotes the time derivative with the referential coordinate(ξ) and $(v_i - \hat{v}_i)f_{,\xi_i}$ represents the convection term due to the relative motion between the material and the mesh. In particular $\hat{\mathbf{v}} = 0$, i.e., $\xi = \mathbf{x}$, the familiar material time derivative is obtained. On the basis of equation (1) ALE formulations on the finite element methodology are derived. Refer Liu et al. (1988) in details.

There are two categories of the ALE analysis for large penetration; i.e., transient analysis and steady-state analysis. As shown in Fig. 1 (a), the transient analysis models downward penetration of the cone penetrometer. On the Lagrangian boundaries, the mesh follows the material and the mesh for soil layers is remapped by adaptive meshing which reduce the distortion of the mesh more than that by the pure Lagrangian analysis with the formulation of large deformation.

The steady-state penetration is analyzed by upward flow of soils into or out of the mesh from bottom to top. The Eulerian boundaries in Fig. 1 (b) are fixed in the spatial coordinate while slightly adaptive meshes are remapped with those boundaries.

As an example cone penetration into homogeneous layer of soft clay was analyzed on the basis of arbitrary Lagrangian-Eulerian (ALE) method. The transient analysis and the steady state analysis were performed respectively by the downward displacement of the cone and the upward flow of soil layer until very large penetration of around 5 times cone diameter. For the solution accuracy smooth load-time function was utilized. The mesh has 4-noded elements with reduced integration and the number of elements is 9,060. The cone was modeled by rigid body in which the radius R=17.9mm, tip length=30.0mm and tip angle=60°. There are contact surfaces between soil and the cone which simulate the interactions such

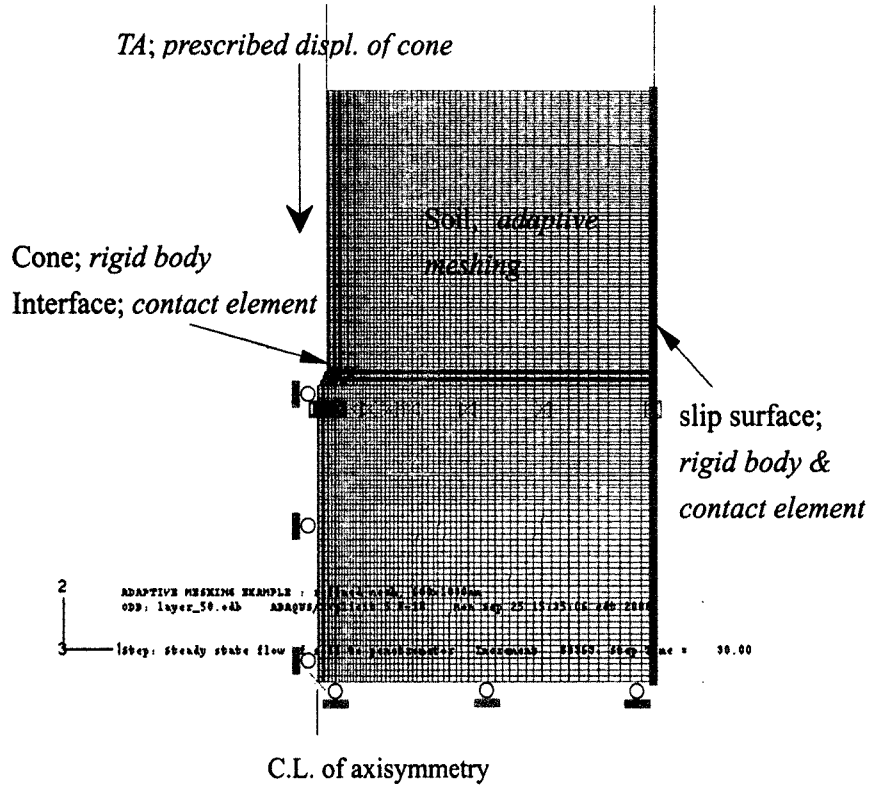

(a) Transient analysis

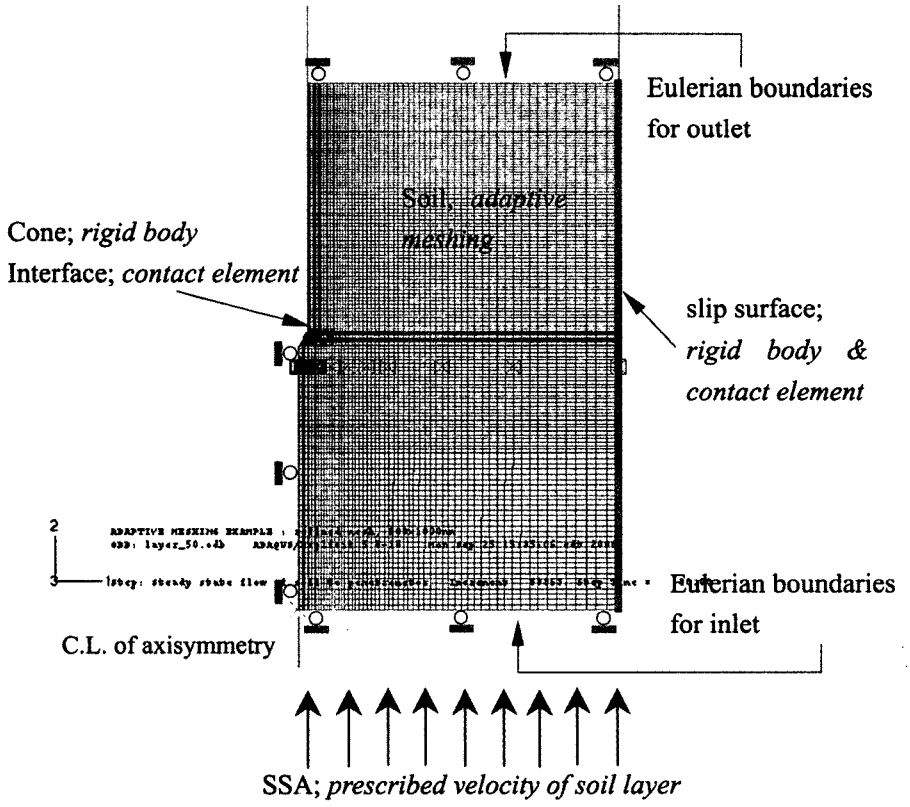

(b) Steady state analysis

Fig. 1. Axisymmetric model in the analysis of cone penetration

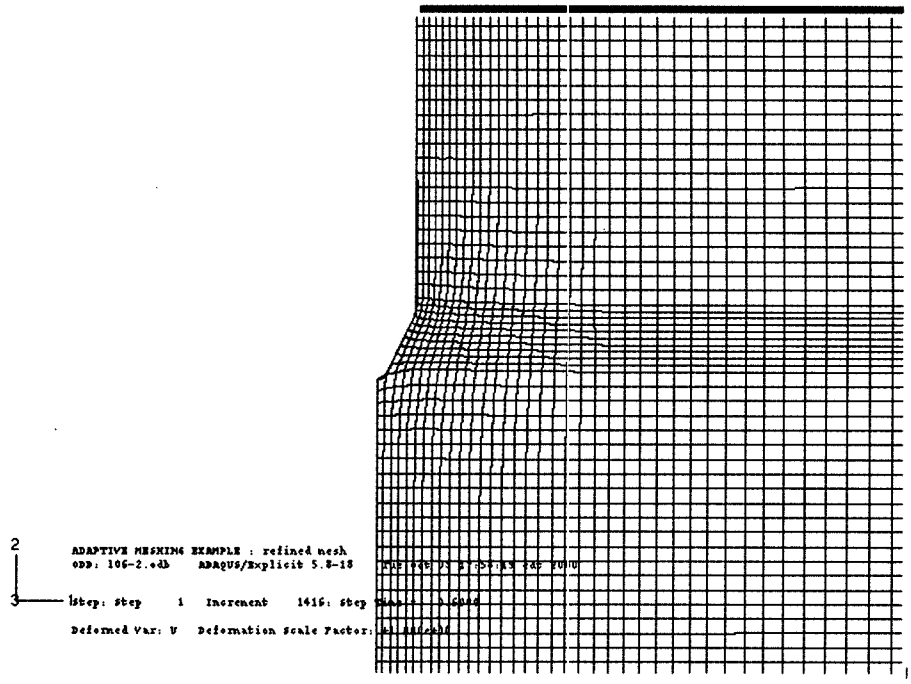

(a) Undeformed mesh

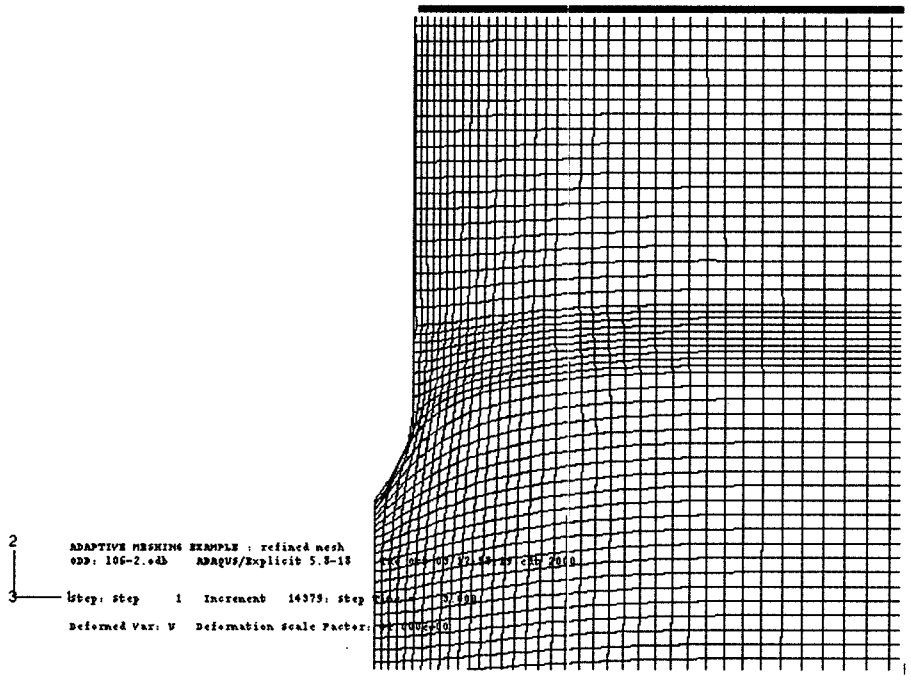

(b) Deformed mesh

Fig. 2. Undeformed and deformed meshes in transient analysis

as slip or friction between surface pairs in ABAQUS.

An elastic-perfectly plastic model with Mises criteria modeled the soil and the parameters were similar to van den Berg's (1996); i.e., Young's Modulus E=3000kPa, Poisson's ratio υ=0.49 and the undrained strength C_u= 20kPa. Soil-cone interaction was considered to model slip in the contact surfaces (no friction or adhesion) and the layer did not have initial stresses.

Fig. 2 (a) shows the undeformed configuration, which is almost the same as the deformed configuration after the steady state analysis. As a result of the transient analysis the deformed configuration after the penetration

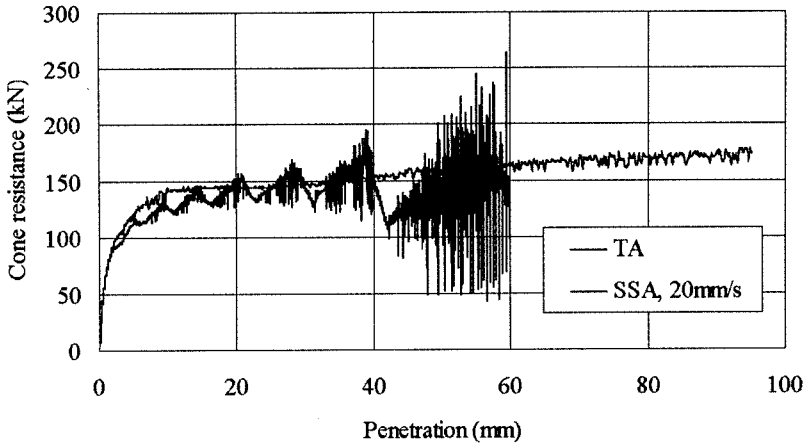

(a) Cone resistance with respect to penetration displacement

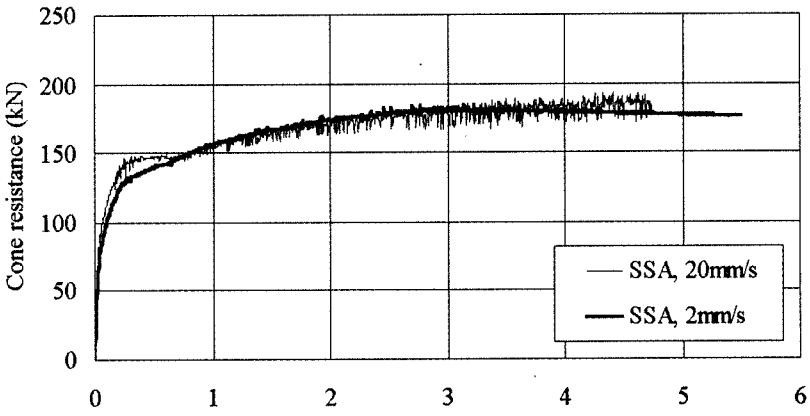

(b) Cone resistance with respect to penetration ratio

Fig. 3. Resistance-displacement relationships

of 1.8 times the cone diameter is shown in Fig. 2 (b). The mesh around cone tip is severely distorted and the following penetration made it impossible to get the numerical solution even in the ALE analysis.

The cone resistance with respect to penetration is shown in Fig. 3. The result of TA(transient analysis) shows that the oscillation of numerical solution occurs from around 10mm penetration and that after the penetration of tip length(30mm) the resultant resistance cannot reach the ultimate value because of severe mesh distortion. However, the SSA(steady state analysis) provides the full relationship of the cone resistance and the penetration depth, while the solution also oscillates slightly. As a result it is found that SSA is better than TA for the evaluation of ultimate resistance in the large penetration analysis.

Fig. 3 (b) shows SSA results with different rates of upward soil flow, 20mm/s and 2mm/sec. The ultimate resistances are almost independent of the rate, while slower rates make less oscillation of the numerical solution. This rate effect did not result from material properties but from numerical accuracy in ABAQUS/ Explicit. As a result it was found that numerical solutions are reliable in the engineering point of view.

3. Example 1: Penetration in Homogeneous Clays

The soil was modeled using an elastic-perfectly plastic model with Mises criteria and the parameters are described in Table 1. In these examples Poisson's ratio ν=0.49 for incompressibility and the undrained strength C_u=20kPa.

Table 1. Material parameters in example 1

run	E (kPa)	C_u (kPa)	a (kPa)	E/C_u
clay_1	3000	20	0	150
clay_2	6000	20	0	300
clay_3	12000	20	0	600
clay_4	30000	20	0	1500
clay_5	6000	20	10	300
clay_6	6000	20	20	300

Soil-cone interaction was considered in *clay_5* and *clay_6*, in which the adhesion a models the perfectly plastic constitutive relationship in contact surfaces. The layer did not have initial stresses.

The mesh is the same as in Fig. 1 (b). The penetration of cone was analyzed on the basis of arbitrary Lagrangian-Eulerian (ALE) method and the steady state analysis was performed by the upward flow of soil layer (20mm/sec) until very large penetration (30 sec).

For the solution accuracy smooth load-time function was utilized as shown in Fig. 4. As a result of the steady state analysis soil flows through the mesh. The outflow velocity from the top surface is almost the same as the inflow because the soil is incompressible.

Fig. 5 shows the deformed mesh after full penetration

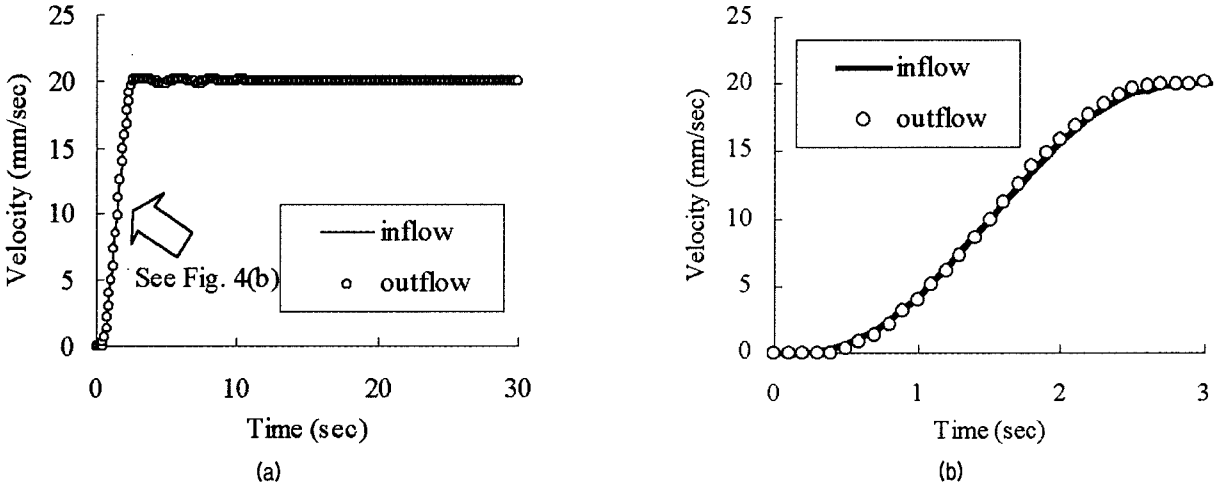

Fig. 4. Velocity-time relationship on the bottom and the top

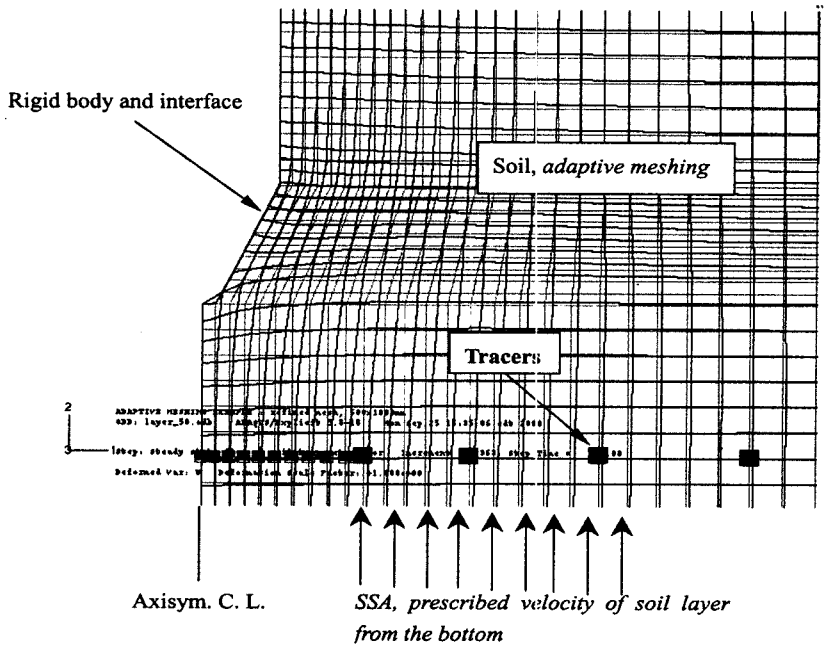

Fig. 5. Deformed mesh after steady state penetration

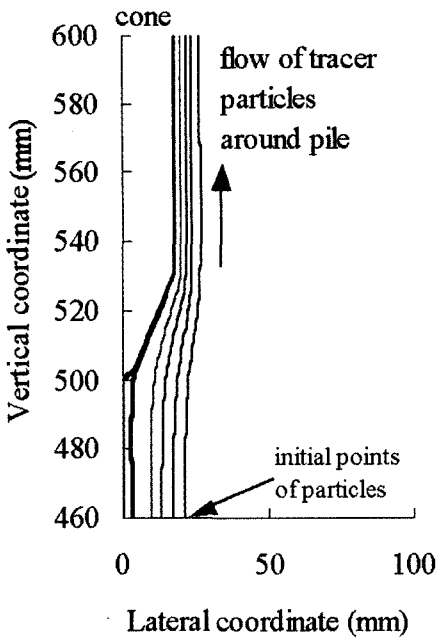

Fig. 6. The flow of particles around cone

(30 sec.), in which the mesh was deformed little even in the steady state analysis. We have tracer particles in order to track node or element variables at flowing material points and to view time history information. Fig. 6 shows (tracer) particle displacement or soil flow around cone for the example *clay_1*. Initial particles were located at 40mm below the cone tip and after 3.5～4.0 seconds the particle arrive at the cone tip. After 5.3～5.6 seconds the particles flow through the surface of the cone tip in Fig. 6.

Let r define initial position of a particle from the center line and R define cone radius. The strain measures of particles are defined in the cylidrical coordinate system as

$$E_1=\varepsilon_{zz},\ E_2=\frac{1}{\sqrt{3}}(\varepsilon_{rr}-\varepsilon_{\theta\theta}),\ E_3=\frac{2}{\sqrt{3}}\varepsilon_{rz} \qquad (2)$$

where ε_{rr}, $\varepsilon_{\theta\theta}$ and ε_{zz} are normal strain components in the $r\theta z$ coordinate and ε_{rz} is a shear strain component in the rz plane. Each strain components are of true (logarithmic) strain measure. The three deviatoric strain components are convenient to descibe the shearing modes in axisymmetric problems, in which the strain measure is based on logarithmic strain. Conventional triaxial tests impose E_1 type of strain and $E_2=E_3=0$, pressuremeter tests apply E_2 and simple shear tests impose E_3 modes (Baligh 1985).

For the points close to the cone, the deviatoric strain paths in Fig. 7 were obtained by tracer particles which indicate that (1) the strain levels are much greater than those normally imposed in common laboratory and pressuremeter tests and that (2) in reaching the final state of strain behind the tip the strain components show significant reversals. These responses are similar trend to 'Strain Path Method' (Baligh 1985) while the closer region to the centerline has less accurate solution at integration points because of mesh refinement.

The reactions of the cone are shown in Fig. 8 (a) and (b) with respect to time and relative displacement of the cone. The solution has some numerical oscillations since ABAQUS/Explicit performs explicit time integration, which can be reduced by finer mesh refinement. Note that the soil layer is homogeneous and interface between soil and cone has no adhesion in these examples. The ultimate resistance occurs after around 200mm penetration or 5 times the cone diameter and increases with E/C_u ratio where E is Young's modulus.

The examples, *clay_5* and *clay_6* included soil-cone adhesion in homogeneous clay and the reaction is compared in Fig. 9 (a) and (b). Even after the penetration

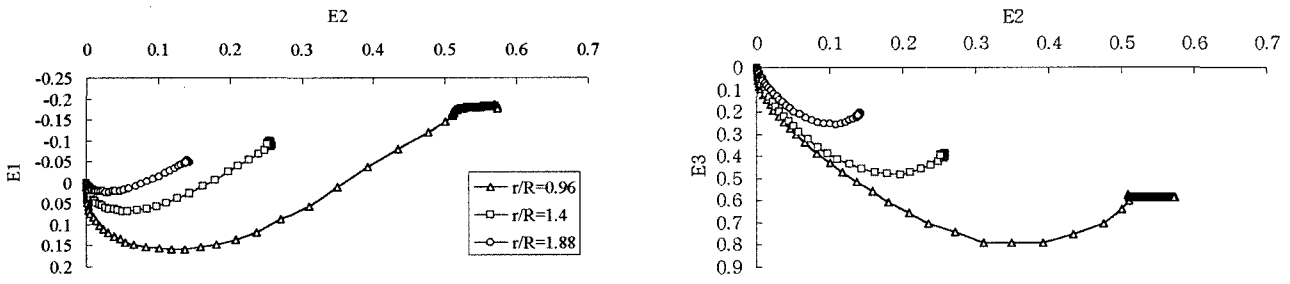

Fig. 7. Strain history of soil particles

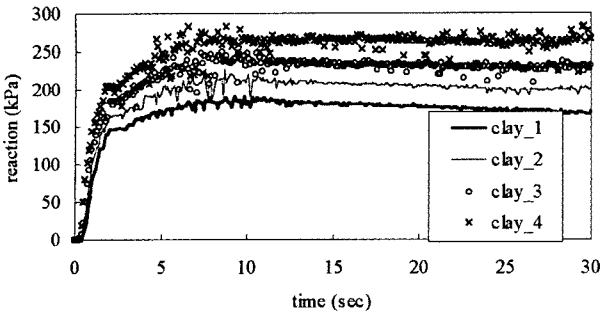

(a) Reactions with time

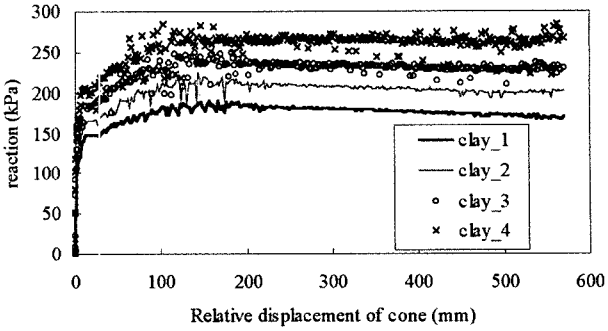

(b) Reactions with displacement

Fig. 8. Cone reactions in the homogeneous layer (no adhesion)

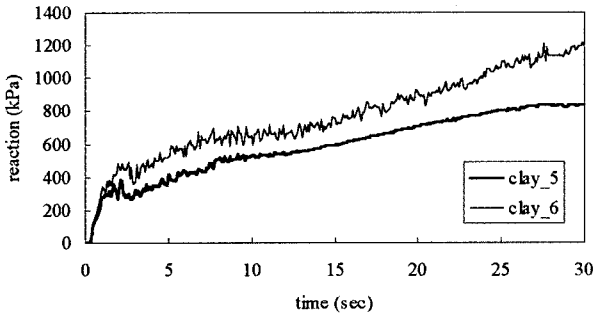

(a) Reactions with displacement

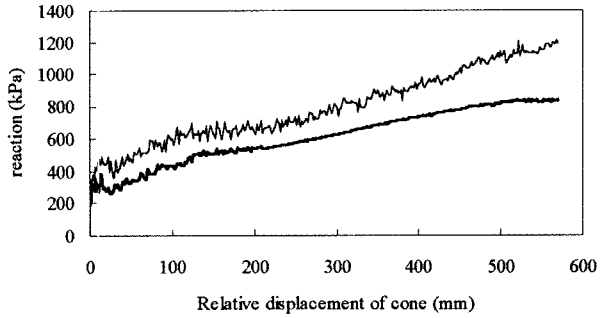

(b) Reactions with displacement

Fig. 9. Cone reactions in the homogeneous layer (adhesion included)

of around 15 times diameter the resistance cannot reach the ultimate value, since the analysis simulates the penetration from surface to such a depth. For the simulation of the actual cone penetration, the length of cone and the test depth specified in soil should be considered, which was beyond the scope of this study. The reaction with adhesion is much larger than those of the slip case. The result is summarized in Table 2.

We can define the cone factor as

$$N_c = \frac{q_c - \sigma_{v0}}{c_u} \tag{3}$$

In the above equation q_c is the axial resistance per unit area at tip, which is provided by the ALE analysis without adhesion. σ_{v0} is the initial vertical stress, which is ignored (or assumed as zero) in these analyses. The cone factor

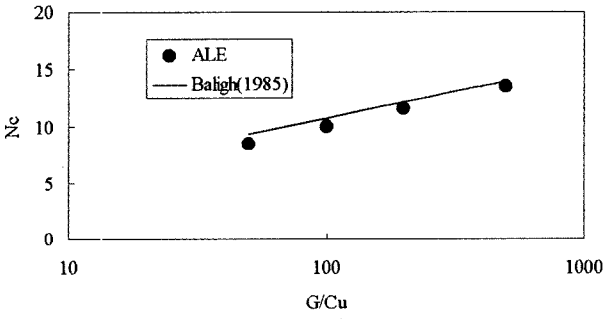

Fig. 10. A comparison for the results of ALE analyses

Table 2. Summary of results in example 1

run	E (kPa)	C_u (kPa)	a (kPa)	ultimate capacity (kPa)
clay_1	3000	20	0	170
clay_2	6000	20	0	200
clay_3	12000	20	0	230
clay_4	30000	20	0	270
clay_5	6000	20	10	more than 840
clay_6	6000	20	20	more than 1190

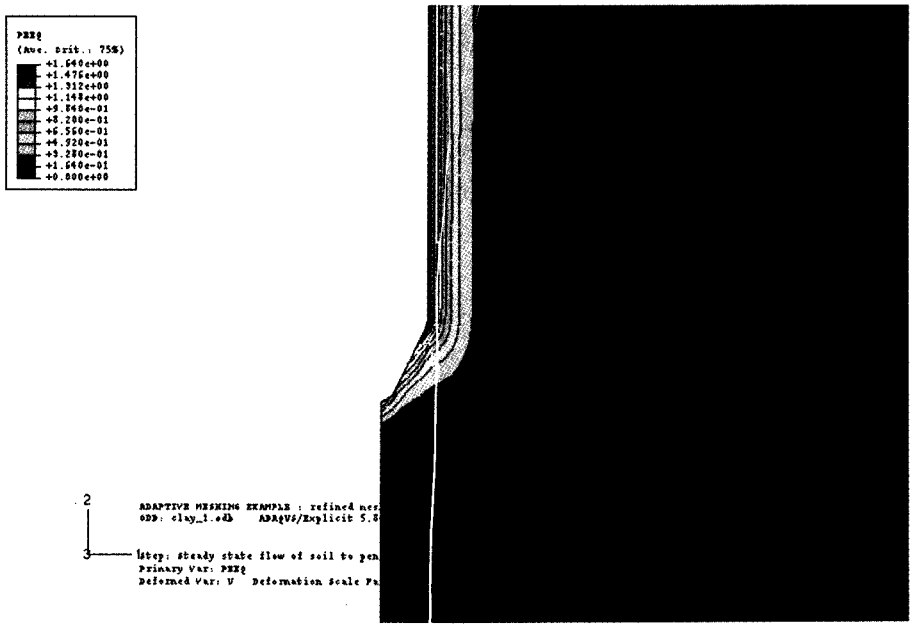

Fig. 11. Plastic strain contour at t=30sec (clay_1)

with respect to G/C_u is shown in Fig. 10 and the result of ALE analyses agrees well with the Baligh's suggestion (1985) that $N_c = 2(1 + \ln(G/c_u)) - 0.49$.

Fig. 11 shows the contour of plastic strain invariant $\bar{\varepsilon}^{pl} = \int \sqrt{\frac{2}{3} d\varepsilon^{pl} : d\varepsilon^{pl}}$ in which we can imagine the zone of zero-plasticity. In the case of *clay_1* to *clay_4* contours of plastic strain for homogenous clays are very similar each other and seem to be independent of soil properties. These are similar to results from strain path method such as the strain path during cone penetration is somewhat independent of soil properties (Baligh 1985). The cases of *clay_5* and *clay_6* (with adhesion) have similar trend but higher strain (distortion) at interface, which results from the different mechanism between cone and soil interfaces.

4. Example 2: Penetration through layered clays

In ABAQUS/Explicit, the boundary between two different materials can never flow through the mesh. Hence, steady state penetration through layered system was performed using the user material subroutine, VUMAT.

The author had to code all constitutive routines in a VUMAT, which makes multi-layers a single material layer in running ABAQUS. However each layer has different parameters or constitutive relationships in a VUMAT. In the analysis of soil flow, the boundary of material or the initial position of materials have to be obtained since the material flows through the mesh. Note that VUMAT can recognize field variables, i.e., material point coordinate and time step. VUMAT makes the mesh region divided by the initial material coordinate, saves as a state variable at the initial stage and with that state variable, selects an appropriate constitutive relationship in the procedure of analysis.

The procedure to describe a VUMAT is as follows: (1) save initial material coordinate on depth as a state variable, (2) select the corresponding layer and parameters and (3) run Mises elasto-plasticity routine which was provided in ABAQUS example code. See Table 3. Actual soil behavior can be modeled with more complex constitutive models than Mises model but advanced constitutive modeling is beyond the scope of this study.

The mesh and numerical model are the same as example 1 in section 3 while soil properties are shown for a series of examples 50~53 in Table 3. The cases of example 52 and 53 have a homogeneous layer of relatively soft and stiff properties. Example 50 has soft

Table 3. Algorithm of VUMAT for the analysis of layered system

```
Read parameters for each layer

Save the set of parameters of the first layer to Parameter Set 1
Save the set of parameters of the second layer to Parameter Set 2
Save the initial vertical coordinate of boundary of two layers to h_ref

If time step equal initial step, then
      Read the initial vertical coordinate of material point from field data
      Save it to state variable on depth
else
      Read the initial vertical coordinate of material point from state variable on depth
endif

If state variable on depth is greater than h_ref, then
      Select Parameter Set 1
Else
      Select Parameter Set 2
Endif

Run the routine for Misses model
```

Table 4. Material parameters in example 2

run	E (kPa)	C_u (kPa)	description
50	2000/5000	10/20	soft/stiff
51	5000/2000	20/10	stiff/soft
52	2000	10	stiff layer
53	5000	20	stiff layer

clay in the upper layer and stiff clay in the lower layer where the boundary is located at 100mm below the tip. In the example 51 the stiff layer is in the upper side and soft layer in the lower side with the same location of boundary as the example 50. Poisson's ratio ν=0.49 and initial stresses and soil-cone interaction are ignored.

As a result of arbitrary Lagrangian Eulerian (ALE) method the reaction per unit area is shown in Fig. 12. The example 52 and 53 shows the reference of cone reaction in soft and stiff homogeneous layers. In example

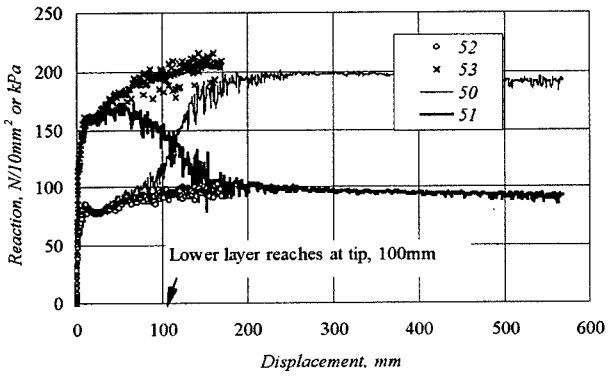

Fig. 12. Reactions at cone in the layered soils

50, the cone has penetrated initially the soft layer and the cone reaction follows the stiff homogeneous layer's. Before cone tip arrive the boundary of two layers (100mm below the initial location of the cone tip) the reaction begins to transfer to stiff layer's and arrives at the ultimate resistance of stiff layer's after around 200mm penetration. Example 51 shows the result to be contrary to the example 50.

In these analyses, the boundary of layers flows through the mesh with materials. In the user material subroutine the initial material point was defined as a state variable in each material point and it is possible to distinguish the layer boundary with the contour of initial depths. Fig. 13 (a) shows the contour of a state variable on the initial depth of material in which the boundary of materials is at 100mm below the cone tip. After penetration the boundary flows upward near the top of the mesh.

Fig. 14 shows the contour of q which is defined as

$$q=\left[\frac{1}{2}\{(\sigma_{11}-\sigma_{22})^2+(\sigma_{22}-\sigma_{33})^2+(\sigma_{33}-\sigma_{11})^2\}+3\{\sigma_{12}^2+\sigma_{23}^2+\sigma_{31}^2\}\right]^{1/2} \quad (4)$$

In the above equation, σ_{ij} (i=1,2,3 and j=1,2,3) is the component of the Cauchy stress tensor in the Cartesian coordinate.

Fig. 14 (a) has softer clay in the upper layer than the lower and shows the boundary of stress distribution and

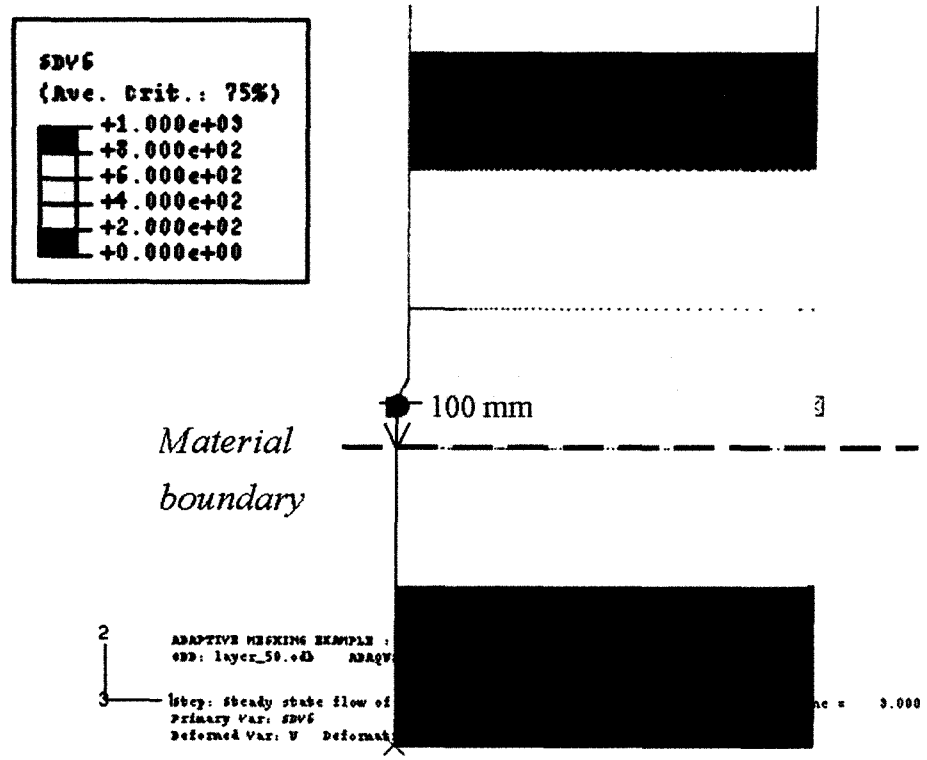

(a) t=3.0 (almost initial condition)

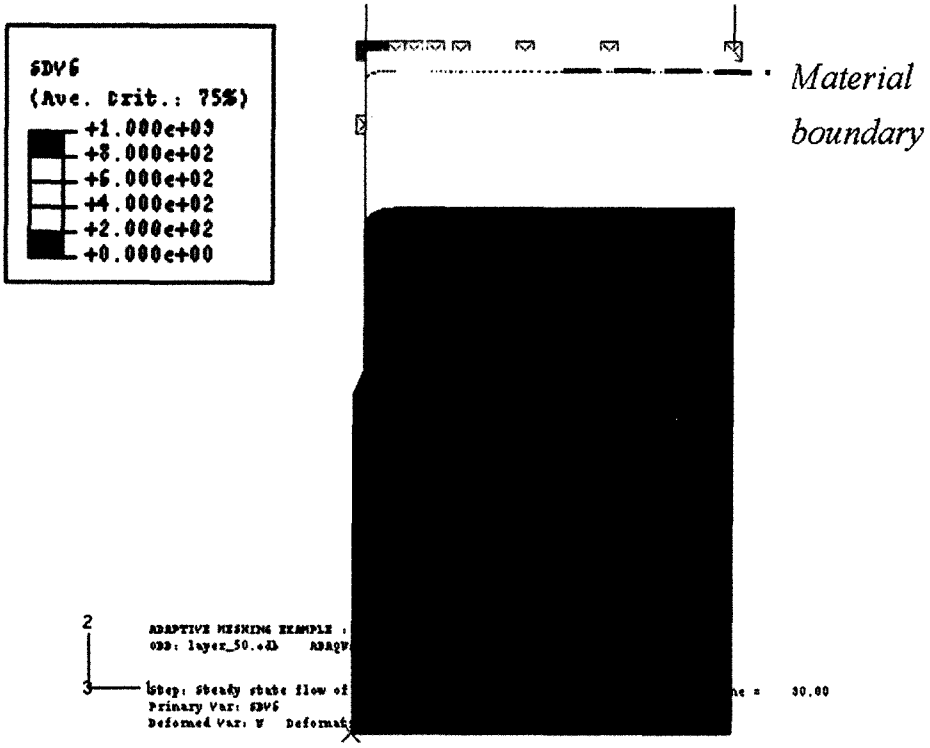

(b) t=30.0 final condition

Fig. 13. State variable on initial position

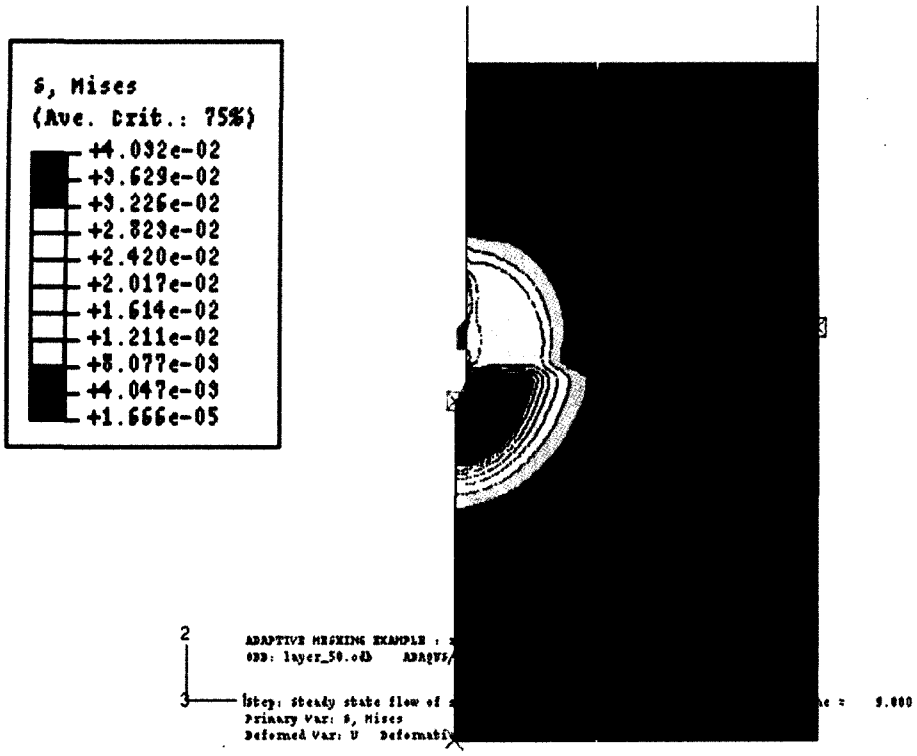

(a) t=9.0

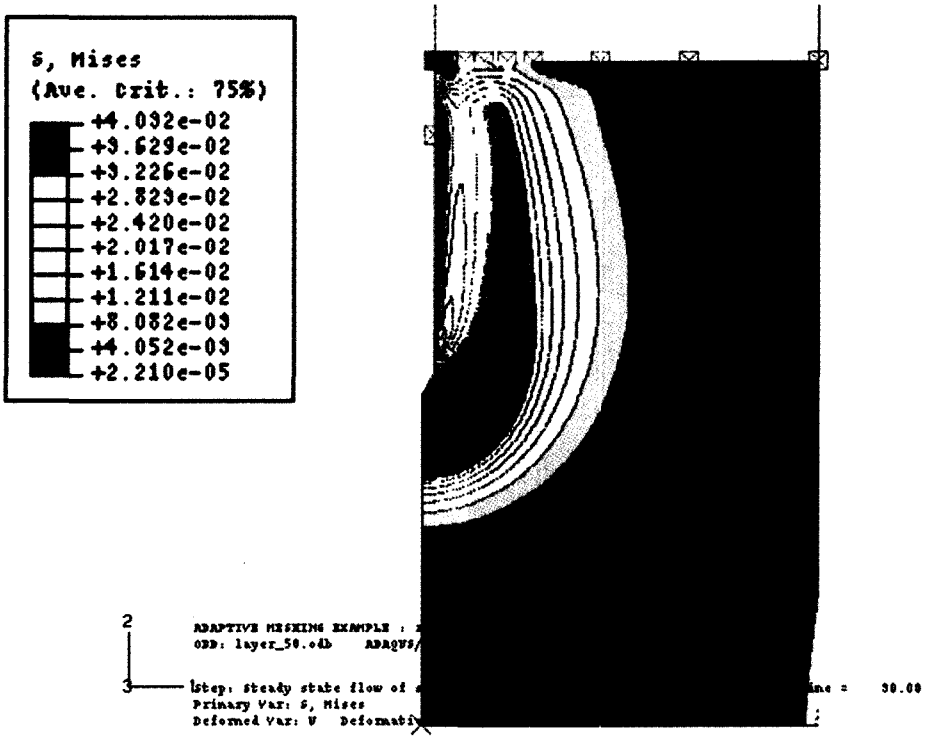

(b) t=30.0

Fig. 14. Deviatoric stress contour of example 50

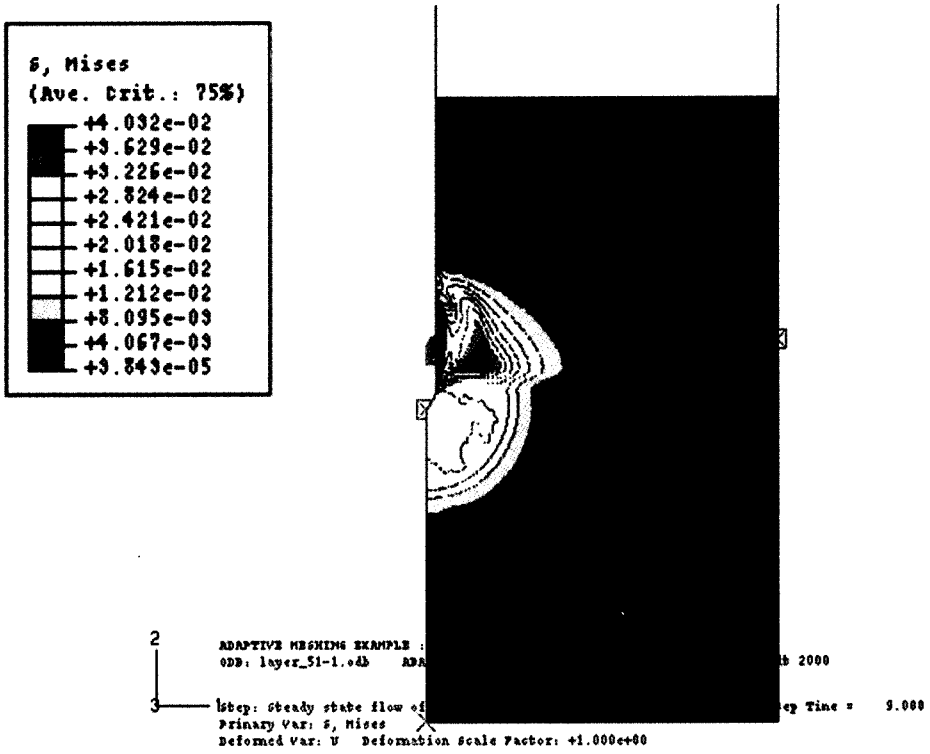

(a) t=9.0

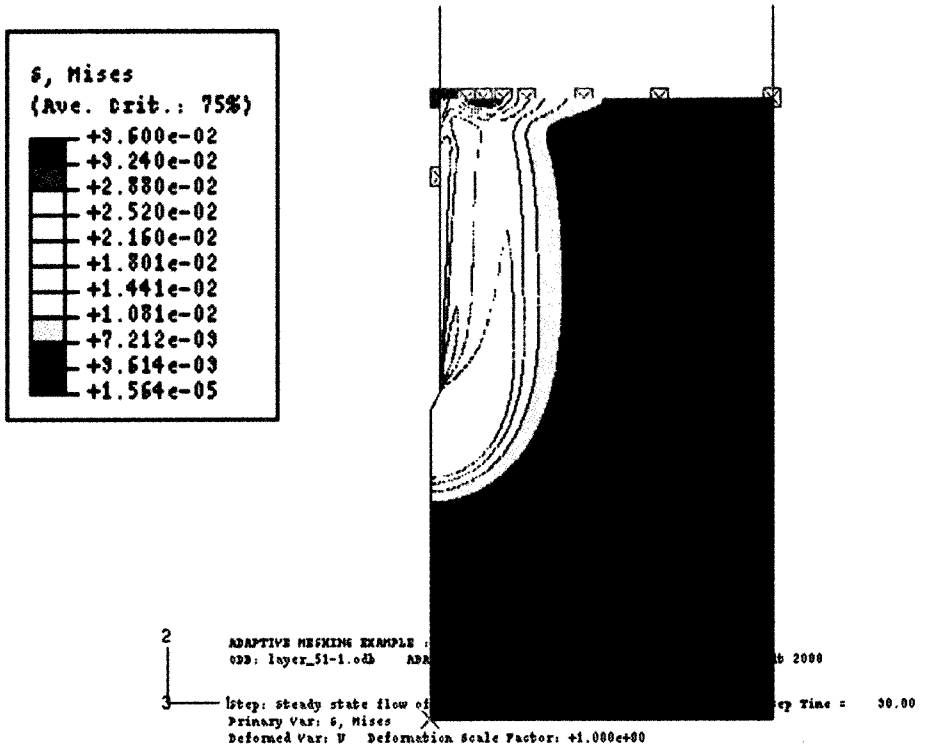

(b) t=30.0

Fig. 15. Deviatoric stress contour of example 51

the lower stiff layer has higher stress concentration near the cone tip. After full penetration the stress distribution is dependent on the strength of the lower clay and most adjacent area near the cone is yielding as shown in Fig. 14 (b). The contrary response is shown in Fig. 15 in which the lower layer is softer than the upper.

5. Conclusion

The Arbitrary Lagrangian-Eulerian analysis was performed for the cone penetration through soils using ABAQUS/ Explicit. The steady state analysis could penetrate to the sufficient depth for simulating full penetration. As a result of the penetration in the homogeneous layer, the paths of soil particles and strain were evaluated which are consistent with the result of strain path method. The ultimate resistance agreed also with the Baligh's solution.

The cone penetration through different soil layers was successfully analyzed with user-defined subroutine, VUMAT in ABAQUS/Explicit. Therefore it is found that the steady state analysis is feasible in penetration analysis through the layered system and that the rigorous analysis of practical penetration problems is readily available with ABAQUS code.

Acknowledgement

Financial support for this research was provided by Korea Science and Engineering Foundation (KOSEF) through Post-Doc support grant.

Reference

1. Baligh, M. M. (1985), "Fundamentals of deep penetration: I. Soil shearing and point resistance," Research Report R85-9, Department of Civil Engineering, MIT.
2. Belytchko, T. (1983), "An overview of semidiscretization and time integration procedures," Computer Methods for Transient Analysis, 1-65, Elsevier.
3. HKS Inc. (1998), ABAQUS/Explicit User's Manual, version 5.8.
4. Kim, D.-K. (2000), "Finite Element Analysis of Piezocone Test I," Journal of the Korean Geotechnical Society, Vol.16, No.4, pp. 183~190.
5. Liu, W. K., Chang, H., Chen, J.-S., and Belytschko, T. (1988), "Arbitrary Lagrangian-Eulerian Petrov-Galerkin Finite Elements for Nonlinear Continua," Computer Methods in Applied Mechanics abd Engineering, 68, pp.259~310.
6. Song, C.-R. (2000), "Estimation of Hydraulic Conductivity Using Piezocone Penetration Test," Journal of the Korean Geotechnical Society, Vol.17, No.2, pp.31~40.
7. Van den Berg, P., de Borst, R., and Huetink, H. (1996), "An Eulerian finite element model for penetration in layered soil," Int. J. for Num. Analt. Methods in Geomechanics, Vol.20, pp.865~886.

(received on Jul. 26, 2001, accepted on Dec. 4, 2001)